TÜBİTAK

Turk J Phys
36 (2012) , 117 – 131.
© TÜBİTAK
doi:10.3906/fiz-1101-88

Nuclear structure of Xe-Pt nuclei in the framework of ARM and odd-even staggering

Harish Mohan MITTAL and Vidya DEVI
Dr B R Ambedkar National Institute of Technology,
Jalandhar-144011, INDIA
e-mails: mittal.hm@lycos.com, vidyathakur@yahoo.co.in

Received: 05.01.2011

Abstract

The asymmetric rotor model (ARM) of collective rotation is used to search for the correlation between the rotational energy with the asymmetric parameter γ_0 for Xe-Pt nuclei. The correspondence of the ratio ROTE/$E(2_1^+)$ vs. $R_{4/2}(= E(4_1^+)/E(2_1^+))$ and γ_0 is used to distinguish between the axially symmetric and triaxial nuclei. The correlation between deformation parameter β and γ_0 is studied to understand the structure of the nuclei. The γ-band energy staggering in low-spin, low-energy spectra of even-even $^{122-124}$Xe and $^{124-128}$Ba nuclei is also discussed. We have compared our results with experimental data and other theoretical models.

Key Words: Asymmetric rotor model, deformation parameters.

1. Introduction

The Bohr-Mottelson expression has been widely used for the description of the low energy spectra of the deformed nuclei that satisfy the rotational limit $R_{4/2} \geq 3.3$ [1]. There are several other formulae that describe the properties of ground band energy of transitional nuclei. The simplest well known expression for rotational spectra is

$$E = \frac{\hbar^2}{2\Im} J(J+1), \tag{1}$$

where $\Im$ and J are the moment of inertia (MI) and spin of nuclei, respectively. The Bohr-Mottelson energy expression for the deformed nuclei [1] is

$$E(J) = AX + BX^2 + CX^3, \tag{2}$$

where $X = J(J+1)$ works only for the well-deformed nuclei having energy ratio $R_{4/2} \geq 3.1$, the rotational limit being 10/3. The anharmonic vibrator model expression [2, 3],

$$E(J) = aJ + bJ^2, \tag{3}$$

is equivalent to the two parameter Ejiri expression [4] of the ground band energy

$$E(J) = (a-b)J + bJ(J+1), \tag{4}$$

which yields a linear relation of $R_{6/2}(= E(6_1^+)/E(2_1^+))$ with $R_{4/2}$ on a Mallmann plot [5]–[6]. However, the experimental data deviates from the linear plot showing the need of a third term i.e. rotation vibration interaction (RVI) term

$$E(J) = aJ(J+1) + bJ + cJ^2(J+1). \tag{5}$$

Here, the first term represents the rotational energy (ROTE), second represents the vibrational (VIBE) energy and the third represents the interaction (INTE) energy. Gupta et al. [7] have studied the effect of rotation on non-rigid nuclear core with the variation of N, Z from a spherical vibrator to an axially deformed rotor. Gupta et al. [5] illustrated the systematic variation of two parts of 2_1^+ state energy with N, Z; e.g., first term $=6a$ is called ROTE, and the sum of VIBE + INTE$= 2b + 12c$ is called the shape fluctuation energy (SFE). The constants a, b and c are calculated by least square fitting method with level up to $J^\pi < 12^+$, below the back bending effect. The correlation of ROTE and VIBE with B(E2) values or β states is such that the energy of 2_1^+ state decreases and increases in a complementary way. Large deviations from these limiting cases occur for the transitional nuclei that cannot be easily explained by any perturbation method, e.g., the $J(J+1)$ expression of level energies of ground band.

Davydov et al. [8, 9] proposed rigid triaxial asymmetric rotor model(ARM) to explain these deviations and obtained better results than the axially symmetric rotational model. The centrifugal stretching term in the $J(J+1)$ expansion of E_J would be smaller if shape asymmetry parameter $\gamma_0 > 0$ was assumed. Gupta and Kavathekar [7] described the interband B(E2) ratios in the rigid triaxial model. The variation of B(E2) with γ_0 is helpful to check the consistency of the model.

Recently, Singh et al., [10] have studied the yrast and γ-band for $^{120-130}$Xe nuclei using ARM by employing the Lipas parameter and commented that the reason of odd even staggering (OES) is the splitting of γ-band in odd and even spin sequence. The structure of the $K^\pi = 2^+$ gamma vibrational bands and the quasi-gamma bands of even Z-even N nuclei is investigated on a global scale. The yrast band energies, OES in the γ-band for Xe (A=116-118) and Ce (A=128,132 and 134) chain have been done in the frame work of Asymmetric Rotor Model [11].

Recently, McCutchan et al. [12] studied the staggering in band energies and the transition between different structural symmetries in nuclei by using the expression

$$S(J) = \frac{\{E(J) - E(J-1)\} - \{E(J-1) - E(J-2)\}}{E(2_1^+)}. \tag{6}$$

In the present work, we try to search whether the $J(J+1)$ rule obeys the three energy sequences of yrast and quasi γ band in Xe and Ba nuclei. Zamfir and Casten [13] examined the values of the staggering indices $S(4,3,2)$ and $S(6,5,4)$ obtained from the experimental data of even-even nuclei and examined whether the nuclei are γ-soft or γ-rigid. Liao [14] had commented that one cannot clearly distinguished between γ-soft and γ-rigid rotor according to the value of $S(4)$. Liao recommended that $S(6)$, $S(8)$ and $S(10)$ should be studied for testing the shapes of nuclei(γ-soft or γ-rigid). Here, we will search whether the $J(J+1)$ rule is obeyed in the three energy sequences of yrast and quasi γ-band. If the rule is obeyed, the nucleus is axially symmetric rotor else it happens

to be triaxial or γ-soft. It should be kept in mind that the indices $\Delta E_1 = E(3_1^+) - (E(2_1^+) + E(2_2^+)) = 0$. This condition is not only valid for the γ-rigid rotor but also for the axial rotor. Both axially symmetric and γ-rigid asymmetric nuclei follow these conditions. Also, ΔE_1 is very small as compared to ΔE_2 for both cases.

1.1. Present approach

If the $K = 2$ band follows the axial rotor model with vibration-rotation interaction, one has the energy spectrum formula

$$E(J) = AJ(J+1) - BJ^2(J+1)^2. \tag{7}$$

If $B = 0$, then $S(J) = 0$ for all values of A in equation (7). If not, one can use the perturbed rotor formula, also known as the soft rotor formula (SRF) [15]

$$E(J) = \frac{J(J+1)}{a(1+bJ)}, \tag{8}$$

where a and b are the constant parameters. The values of a and b are fitted by using 2_γ^+ and 4_γ^+ energies in the even sequence and 3_γ^+ and 5_γ^+ energies in the odd sequence. For these calculations, experimental data is taken from www.nndc.bnl.gov [16].

We also study the variation of the ratios of ROTE/$E(2_1^+)$, VIBE/$E(2_1^+)$ and SFE/$E(2_1^+)$ energy with γ_0 to understand the difference between axially symmetric and triaxial nuclei. We compare the RVI formula with other three parameter formula such as anharmonic vibrator (AHV) formula and VMINS3 model [17], which is the modified version of variational moment of inertia model(VMI) [18], to check the accuracy of this formula. The variation of γ_0 with β is helpful to understand the structure of nuclei.

2. The asymmetry parameter (γ_0)

There are several methods to calculate the asymmetry parameter γ_0. One can calculate γ_0

(a) from the ratio $R_\gamma = E(2_2^+)/E(2_1^+)$ [9];

(b) from the ratio $R_{4/2}$ [19], indicating that the DF model is valid only for those nuclei which have the ratio $R_{4/2}=\frac{10}{3}$ to $\frac{8}{3}$;

(c) from the energy of 4_1^+ and 2_2^+ states [20] and from sum of the absolute $B(E2; 2_1^+ \to 0_1^+)$ and $B(E2; 2_2^+ \to 0_1^+)$ value [21]. In this method, the sum of the absolute B(E2) values are used to determine the value of quadrupole moment Q and γ_0.

Varshni and Bose [19] preferred to determine γ_0 from $R_{4/2}(= E(4_1^+)/E(2_1^+))$, thereby excluding nuclei with $R_{4/2} < 8/3$, for which Van Patter [22] noted the large deviations. Gupta et al., [21] used the B(E2) values to determine γ_0. As these B(E2) values are small and are not easily available with good accuracy, therefore, γ_0 from the level energies should be more reliable. We have derived γ_0 from the R_γ values using the equation that given by Davydov et al. [8]:

$$\gamma_0 = \frac{1}{3}\sin^{-1}\left[\frac{9}{8}\left(1 - \left(\frac{R_\gamma - 1}{R_\gamma + 1}\right)^2\right)\right]^{1/2}, \tag{9}$$

for Z=52–78, N=68–78 and N=84–104. In terms of B(E2) values γ_0 is equal to

$$\frac{B(E2:2_2^+\rightarrow 0_1^+)}{B(E2:2_1^+\rightarrow 0_1^+)}=\frac{\sqrt{9-8\sin^2 3\gamma_0}-3+2\sin^2 3\gamma_0}{\sqrt{9-8\sin^2 3\gamma_0}+3-2\sin^2 3\gamma_0}. \tag{10}$$

From the above relation we have also calculated β. According to the approximate empirical Grodzins relation [23]

$$E(2_1^+)\cdot B(E2;2_1^+\rightarrow 0_1^+)=2.5\times 10^{-3}Z^2A^{-1}\text{ [in units of } e^2b^2\text{MeV]}, \tag{11}$$

hence

$$E(2_1^+)=\frac{2.5\times 10^{-3}Z^2A^{-1}}{B(E2;2_1^+\rightarrow 0_1^+)}\text{ [in units of } e^2b^2\text{MeV]}. \tag{12}$$

On relating β and $E(2_1^+)$ we obtain

$$\beta_G^2\cong\frac{1224}{E(2_1^+)A^{7/3}}, \tag{13}$$

where β_G is a constant. Hence

$$\beta=\beta_G\left(\frac{9-\sqrt{81-72\sin^2(3\gamma_0)}}{4\sin^2(3\gamma_0)}\right), \tag{14}$$

3. Results and discussion

3.1. Variation of ROTE $/E(2_1^+)$ versus $R_{4/2}$

In quadrant-IV, 66 ≤ N ≤ 82 (Xe–Sm), region of neutron deficient nuclei $ROTE/E(2_1^+)$ varies linearly with $R_{4/2}$ ratio and lies between 2.1 and 2.8 (see Figure 1). At $R_{4/2}=2.1$, the $^{130-132}$Xe nuclei behaves like a vibrator SU(5) having low value of $ROTE/E(2_1^+)$ (approximately 35%) and at $R_{4/2}=2.2$ the nuclei attain the E(5) symmetry. The neutron deficient Xe, Ba, Ce, Nd and Sm nuclei having $ROTE/E(2_1^+)=75\%$ are γ-soft and lie between the vibrator and deformed γ-soft structure. This corresponds to SU(5)-O(6) transition region, in the language of the interacting boson approximation (IBA) [24]. Next in quadrant-I, $N>82$, of small neutron number i.e. $N=84-88$, the $R_{4/2}$ ratio of Gd lies between 1.8–2.2, having $ROTE/E(2_1^+)=20\%$. Hence these nuclei are vibrational [SU(5)] in nature. For $R_{4/2}=3.3$ and $ROTE/E(2_1^+)=100\%$ all these nuclei are axially symmetric in nature. In quadrant II, $N<104$ at $N=90$, the Er nuclei behave as γ-soft, having $R_{4/2}=2.4$ and ROTE/ $E(2_1^+)=20\%$. But with increasing neutron number, $R_{4/2}$ increases and deformation also increases hence ROTE/ $E(2_1^+)=100\%$, therefore, these nuclei are example of SU(3) symmetry. Next, in quadrant-III, N>104, Pt nuclei lie below in the curve because at low value of $R_{4/2}(\leq 3.0)$, it is not deformed. At $R_{4/2}=2.9$, there is a critical point symmetry i.e X(5) where second order transition takes place.

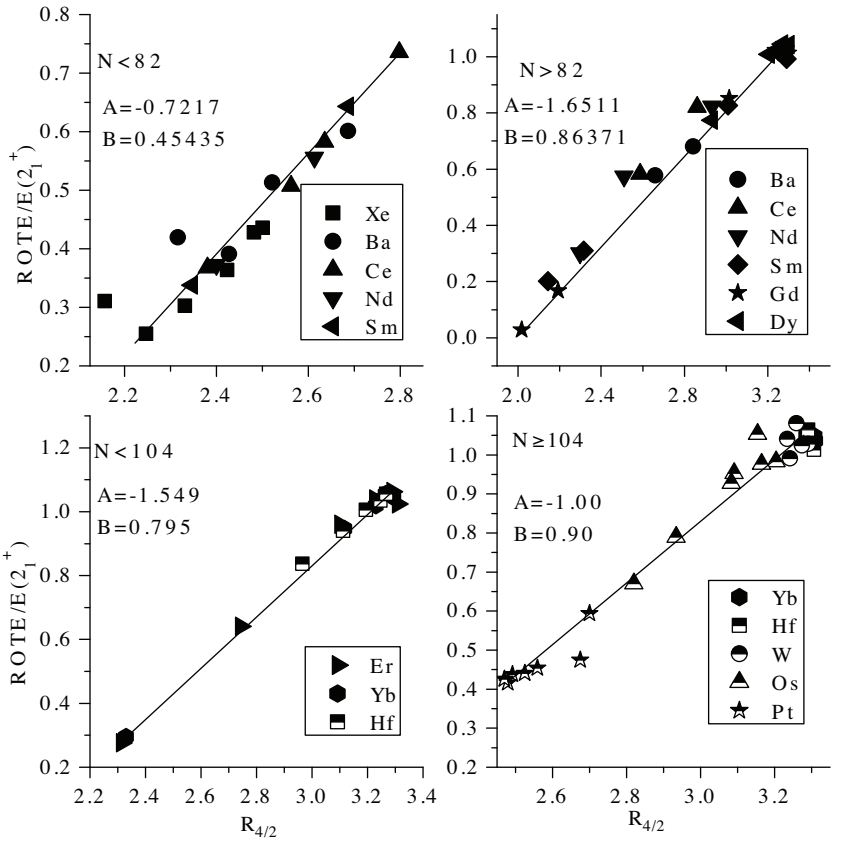

Figure 1. Variation of ROTE/$E(2_1^+)$ as a function of $R_{4/2}$ for $N = 68$–126 in all four quadrants (Q-I-IV).

3.2. Variation of ROTE/ $E(2_1^+)$ versus γ_0

In Figure 2, for $N < 82$ (quadrant-IV), the ratio ROTE/$E(2_1^+)$ for Xe-Sm nuclei shows a monotonic linear fall with increasing γ_0. Here, γ_0 values lies between 22° and 30°, indicating that these neutron deficient nuclei lie in the [SU(5)–O(6)] region, i.e. the γ-soft region where the potential is γ-independent. Even at $\gamma_0 = 22°$ ROTE/$E(2_1^+)$ is approximately 75%, i.e., a large rotational energy at small $R_{4/2}$ (= 2.8). In Sm nuclei for small neutron number, i.e., $N = 82$–86, γ_0 is higher but ROTE/$E(2_1^+)$ energy is small, hence these nuclei lie in the SU(5) region. Next, at $\gamma_0 = 8°$, for ROTE/$E(2_1^+) = 100\%$, Sm, Gd and Dy nuclei are axially symmetric in nature. ^{156}Er nuclei, having $R_{4/2}$= 2.3, lie between E(5) and γ-soft nuclei at lower value of ROTE/$E(2_1^+) \simeq 20\%$. Similarly, at $N = 90$, the relative ROTE/$E(2_1^+)$ is 50% at $R_{4/2} = 2.7$, containing small rotational energy part and behave as O(6) nuclei. But in quadrant II at $N = 92$–102, the value of γ_0 is less but ROTE/$E(2_1^+)$ rises to 100%, hence these nuclei are axially symmetric rotor having $R_{4/2} = 3.3$. For $N \geq 104$ (quadrant III) the datum of Pt nuclei lies below the curve because these nuclei do not get deformed below 16°, hence here value of ROTE/$E(2_1^+)$ is 100%. The behavior of VIBE/$E(2_1^+)$ is opposite to ROTE/$E(2_1^+)$ given by

$$Y_J = \text{ROTE}/E(2_1^+) = B + A[\exp(C \cdot X)], \tag{15}$$

where A, B and C are constant parameters obtained from the curve and X is the x-axis scale factor. The values of fitting parameters are listed in the graphs for all the four regions. In Figures 3 and 4 we see the variation of VIBE/$E(2_1^+)$ with $R_{4/2}$ and γ_0. The VIBE/$E(2_1^+)$ energy decreases for both $R_{4/2}$ and γ_0. Similarly, the SFE/$E(2_1^+)$ energy shows same trend as that of the VIBE/$E(2_1^+)$ energy (see Figures 5 and 6).

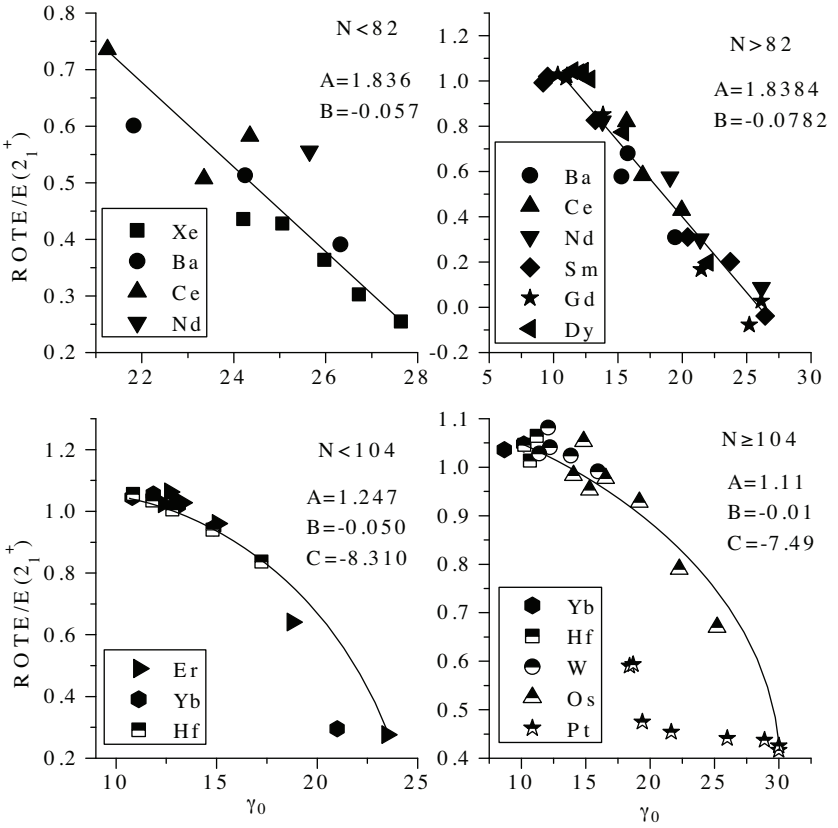

Figure 2. Variation of ROTE/$E(2_1^+)$ as a function of γ_0 for $N = 68$–126 in all four quadrants (Q-I-IV).

3.3. Study of odd-even staggering in $^{122-124}$Xe and $^{124-128}$Ba nuclei

Thiamova [26] studied the staggering of γ-band level energies and compared it with the IBM model. The level energies for the γ-band in $^{122-124}$Xe and $^{124-128}$Ba nuclei have been plotted. In Figure 9 we see the variation of staggering factor $S(J)$ with spin J for ^{122}Xe and ^{124}Xe nuclei. The spacing between odd even spin levels in the present work are in close agreement with experimental values for $S(4)$, $S(5)$ and $S(6)$. For higher values of J, separation increases between evaluated and experimental values of $S(J)$, but in small amounts. In Figure 10 we see the variation of $S(J)$ with J for ^{124}Ba and ^{126}Ba. The calculated value of $S(J)$ matches excellently with the experimental data for $S(4)$ to $S(10)$ factor in ^{124}Ba while a small deviation in $S(9)$ and $S(11)$ is found in ^{126}Ba nuclei. Next we see the variation of ^{128}Ba nuclei in Figure 11. The calculated and experimental values of $S(J)$ shows excellent agreement up to $S(10)$. This means that there is a small energy difference between there energy levels. Next we see the comparison between the experimental and calculated values of the ground band and the gamma band energies.

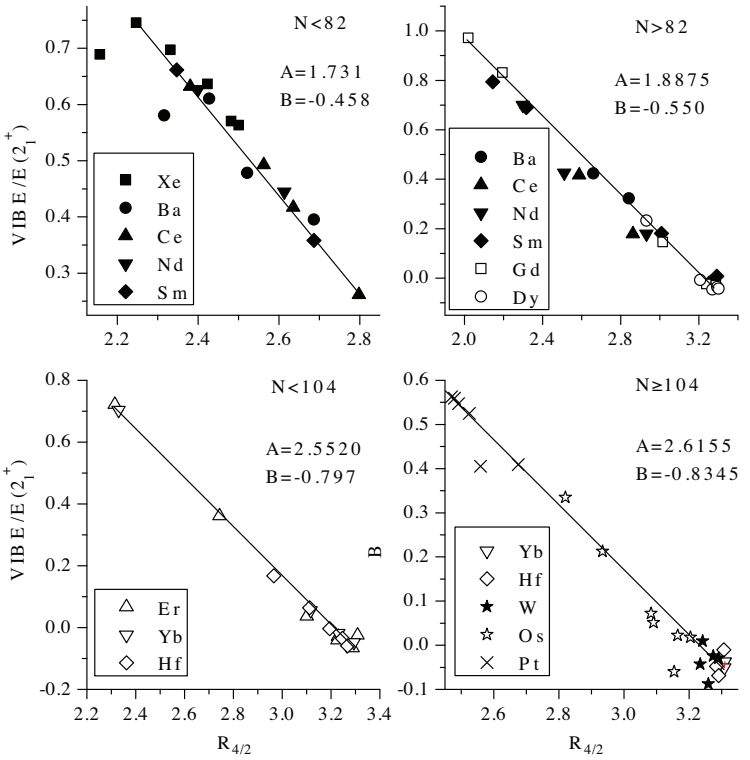

Figure 3. Variation of VIBE/$E(2_1^+)$ as a function of $R_{4/2}$ for $N = 68$–126 in all four quadrants (Q-I-IV).

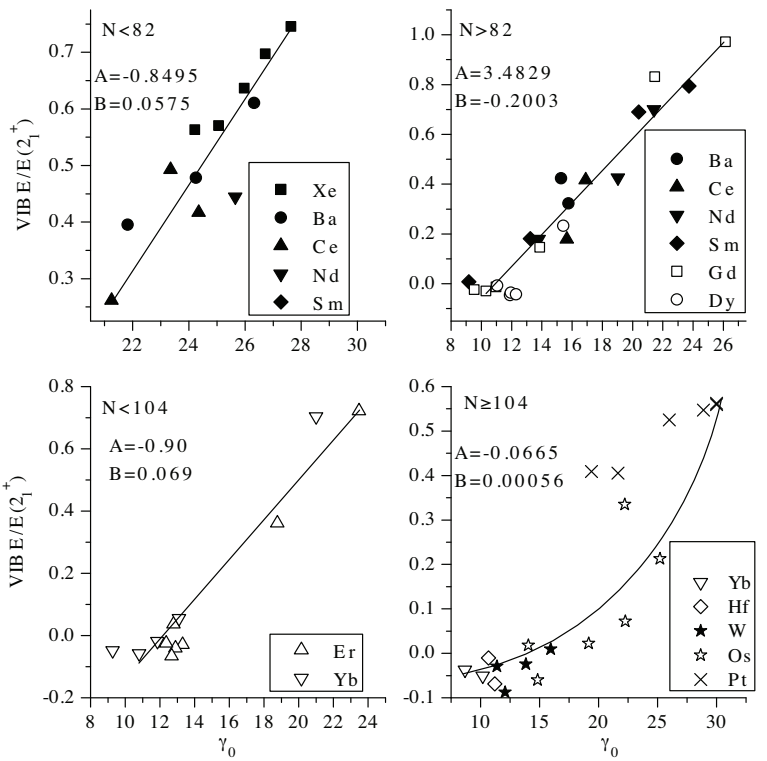

Figure 4. Variation of VIBE/$E(2_1^+)$ as a function of γ_0 for $N = 68$–126 in all four quadrants (Q-I-IV).

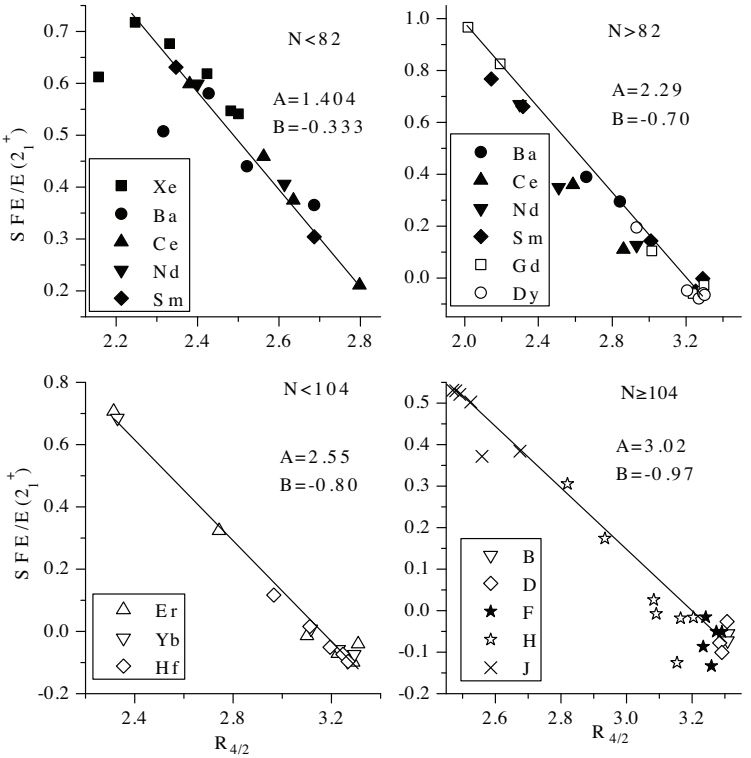

Figure 5. Variation of SFE/$E(2_1^+)$ as a function of $R_{4/2}$ for $N = 68$–126 in all four quadrants (Q-I-IV).

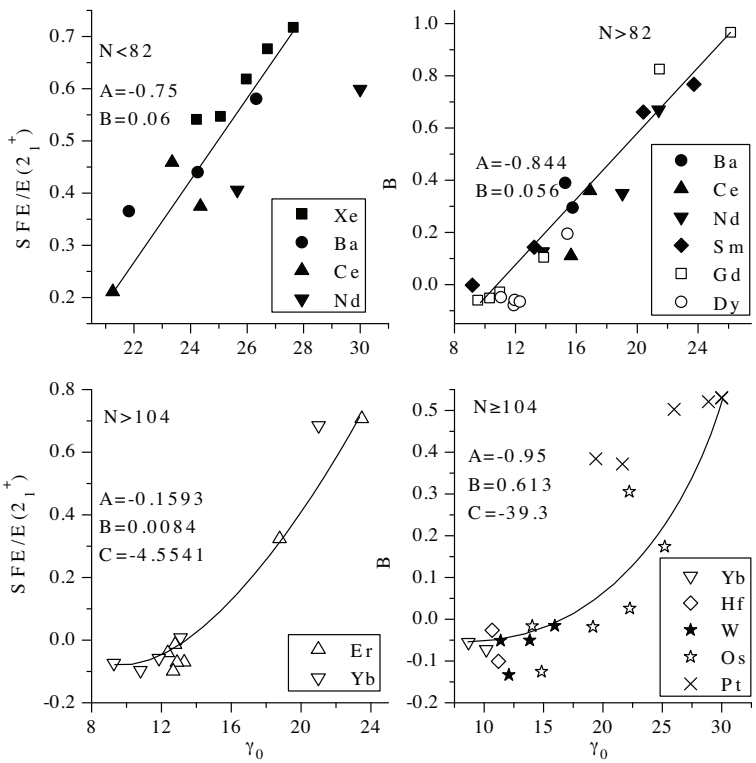

Figure 6. Variation of SFE/$E(2_1^+)$ as a function of γ_0 for $N = 68$–126 in all four quadrants (Q-I-IV).

Figure 7 we see the variation of γ_0 and β. Both these parameters show close correlation. The variation of γ_0 and β for Hf-Pt nuclei are shown by Esser et al. [25]. We also correlate it for the light nuclei and find that the correlation is excellent. Therefore, this variation suggests that β remains constant with γ_0 for soft nuclei as compared to the well deformed nuclei. In Figure 8 we see the variation of γ_0 with boson number N_B. The asymmetric parameter γ_0 is an effective parameter, therefore the study of all the nuclei is worthwhile.

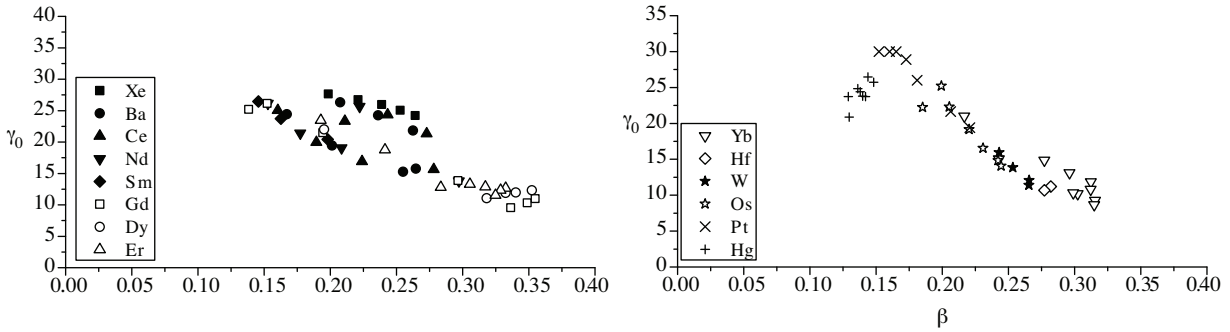

Figure 7. Variation of γ_0 with boson number N_B for $N = 68$–126 region nuclei.

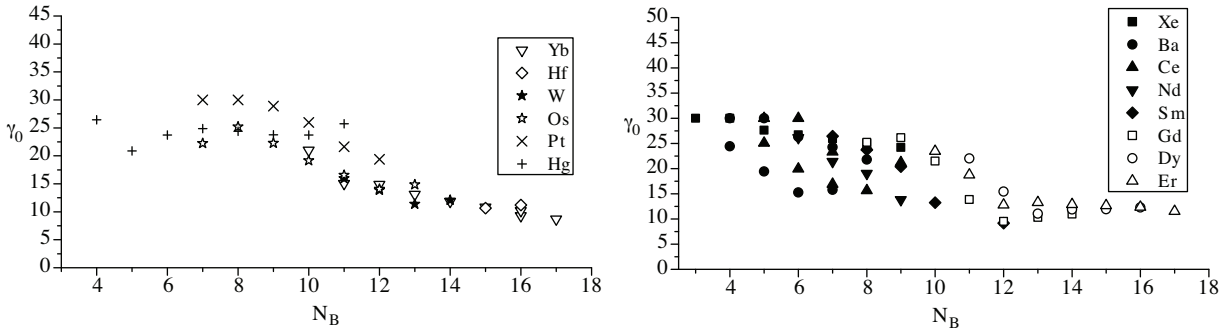

Figure 8. Variation of γ_0 with boson number N_B for $N = 68-126$ region nuclei.

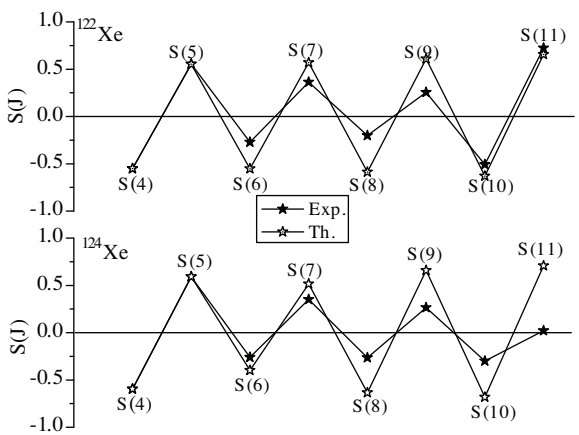

Figure 9. Signature splitting $S(J)$ is plotted versus spin J for $^{122-124}$Xe nuclei.

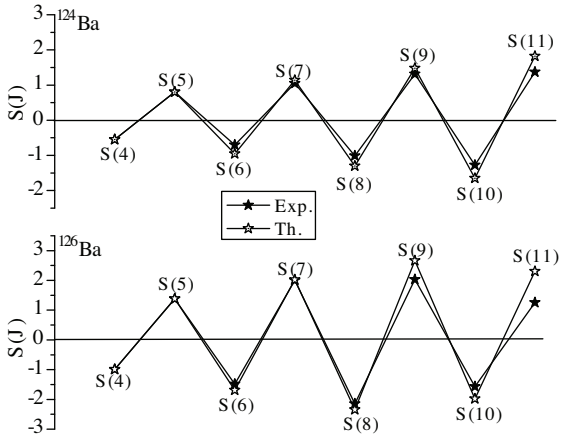

Figure 10. Signature splitting $S(J)$ is plotted versus spin J for $^{124-126}$Ba nuclei.

When we see the variation of $S(J)$ with $R_{4/2}$ (see Figure 12), the even staggering factors $S(4)$, $S(6)$ and $S(8)$ attain negative value and the odd staggering factors such as $S(5)$ and $S(7)$ have positive values. The ratio $R_{4/2}$ lies between 2.4–2.9, which means nuclei are in the range of O(6) and X(5) symmetry. When $R_{4/2}$ is 2.4, $S(4) = -0.5$ and $S(5) = 0.5$, in the case of Ba nuclei. As $R_{4/2}$ approaches X(5) symmetry, the value of $S(8)$ becomes equal to -2.8, which is the minimum value; but on the other side, for the same $R_{4/2}$, $S(7)$ attains maximum value of staggering factor, i.e $S(J) = 2.3$.

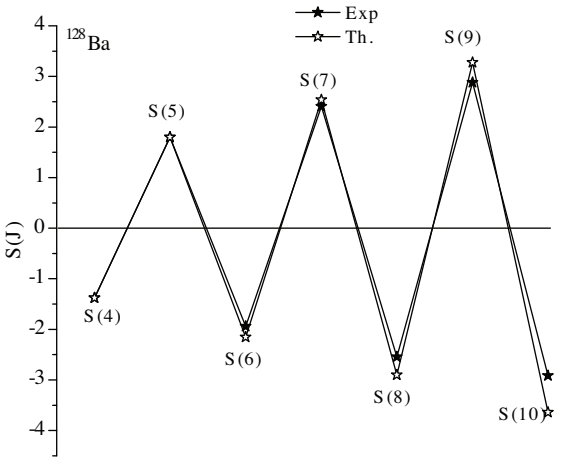

Figure 11. Signature splitting $S(J)$ is plotted versus spin J for ^{128}Ba nuclei.

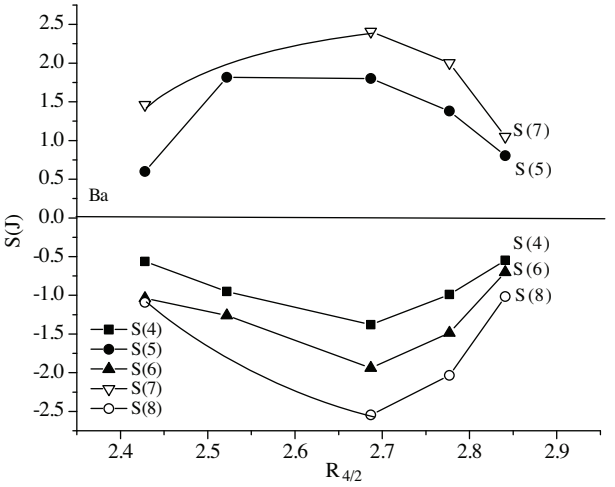

Figure 12. The experimental $S(J)$ as a function of $R_{4/2}$ for Ba nuclei.

In Figure 13 we plot the $^{122-124}$Xe nuclei, which shows good agreement up to $J = 8^+$. Beyond this there is a fall in the calculated energies. In the case of gamma band, a close agreement is found up to $J = 5^+$ after which there is fall in gamma band energies. Next we compare the calculated and experimental values for $^{124-126}$Ba nuclei. The ground band energy shows close agreement up to $J = 8^+$ similar to that of Xe nuclei. But in case of gamma bands the agreement is good up to $J = 11^+$ for ^{126}Ba nuclei and $J = 10^+$ for ^{124}Ba nuclei (see Figure 14). We took another test of triaxiality on the basis of energy relation $\Delta E_1 = E(3_1^+) - \left[E(2_1^+) + E(2_2^+)\right]$ for triaxial nucleus and $\Delta E_2 = E(3_1^+) - \left[2E(2_1^+) + E(4_1^+)\right]$ for γ-soft nucleus given by Wilets and Jean[27]. A large value of ΔE_1 and small value of ΔE_2 reflects a γ-soft character. The difference ΔE_1 is low while ΔE_2 is large for $^{122-124}$Xe which reflects the triaxial nature. For $^{124-128}$Ba , ΔE_1 is large and ΔE_2 is small which show the γ-soft nature. The values of ΔE_1 and ΔE_2 are presented in Table.

Table. The experimental and calculated difference ΔE_1 and ΔE_2

Nuclei	^{122}Xe	^{124}Xe	^{124}Ba	^{126}Ba	^{128}Ba
Exp.ΔE_1	40.04	46.1	60	106	157
Exp.ΔE_2	275.72	339.2	51	13	5
Th.ΔE_1	48.6	46.1	59.3	106.6	155.9
Th.ΔE_2	226.4	339.2	51	12.7	6.8

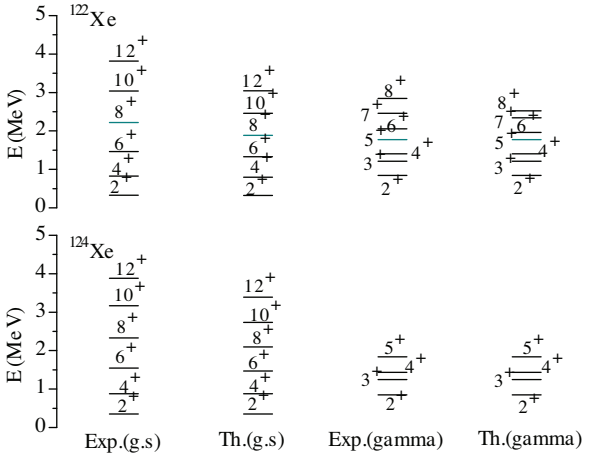

Figure 13. Comparison between experimental and calculated g-band and γ-band energy of $^{122-124}$Xe nuclei.

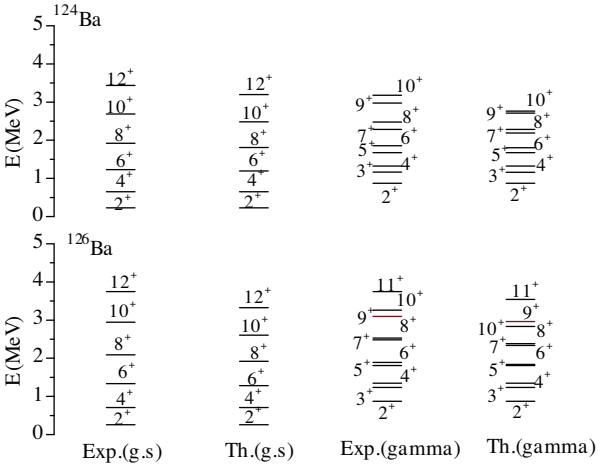

Figure 14. Comparison between experimental and calculated g-band and γ-band energy of $^{124-126}$Ba nuclei.

3.4. Comparison with three parameter formulae

In this subsection we show a comparison of present work (RVI) with other formulae such as AHV and VMINS3. In Figure 15 we have taken $^{120-122}$Xe, ^{126}Ba and ^{152}Sm nuclei. The present work shows good agreement with the experimental energy up to 14^+ ground energy level. In Figure 16 we have taken ^{162}Dy, ^{164}Yb, ^{172}Hf and ^{174}W nuclei. This graph shows that the present work is as equivalently good as the other formulae.

4. A Comparison with other model equation

In this section we discuss how equation (4) is related to other formulae used in the present calculations. Holmberg and Lipas [28] noted that the Moment of Inertia $\Im$ of the deformed nuclei increase with level energy E linearly,

$$\Im(J) = a + bE, \tag{16}$$

and obtained a two parameter ab formula by using equation (1) and equation (16):

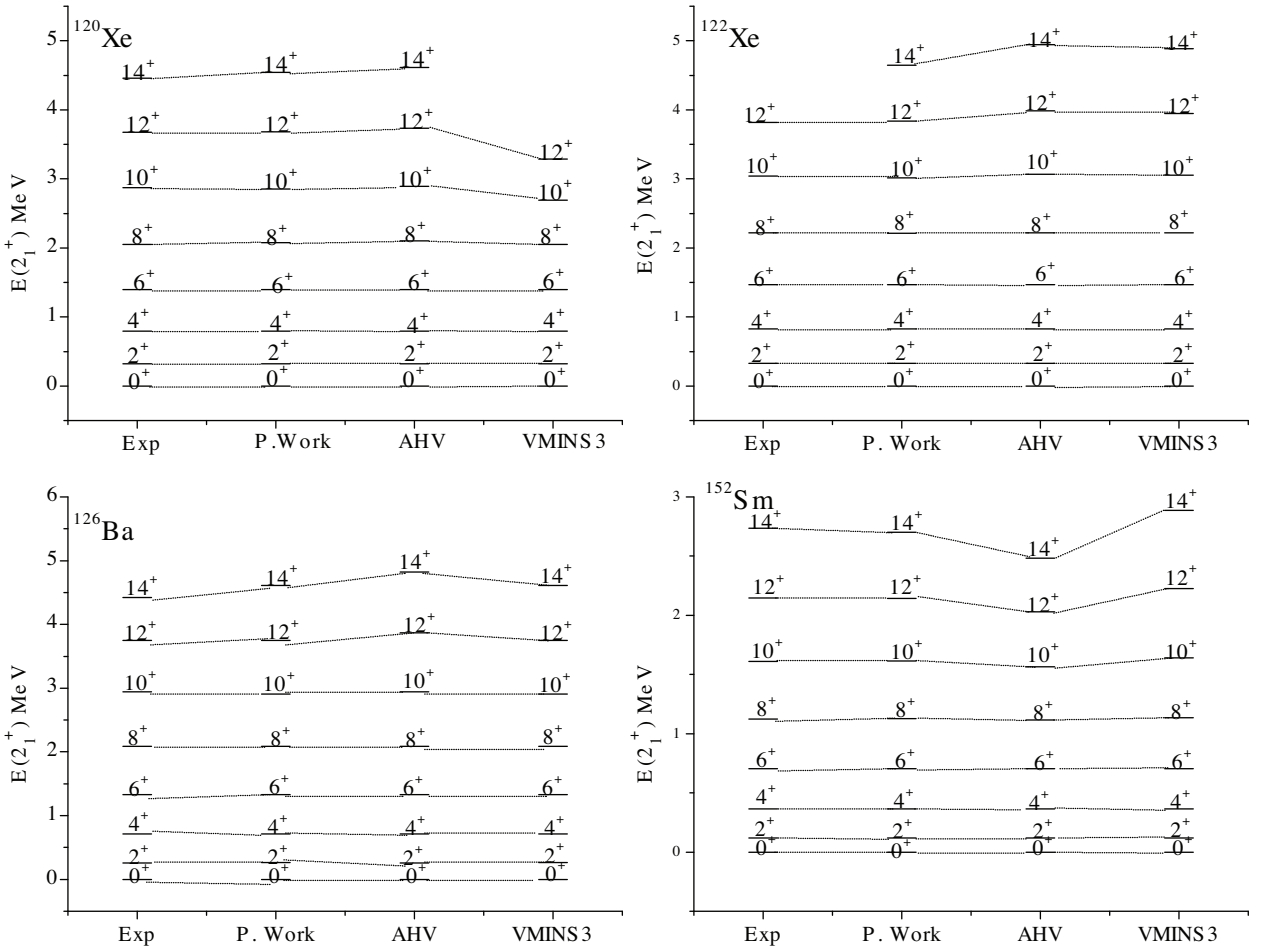

Figure 15. Comparison between experimental energy with anharmonic vibrator expression (AHV), VMINS3 model and p. work.

$$E(J) = a\left[\sqrt{1 + bJ(J+1)} - 1\right]. \tag{17}$$

Later, Zeng et al. [29] illustrated the non linearity relation between $\Im$ and E in the rotational spectra for low and high spins. However, they derive a new relation between $\Im$ and E,

$$\Im = \frac{1}{2ab}\left(\sqrt{1 + \frac{2}{a}E} + 1\right), \tag{18}$$

by using equations (1), (17), (18) and formulated a new energy expression called the pq formula:

$$\begin{aligned} E(J) =& a\left(\left\{\left(\frac{bJ(J+1)}{2}\right)^2 + \left[\left(\frac{bJ(J+1)}{2}\right)^4 + \left(\frac{bJ(J+1)}{3}\right)^3\right]^{\frac{1}{2}}\right\}^{\frac{1}{3}}\right. \\ &\left. + \left(\left\{\left(\frac{bJ(J+1)}{2}\right)^2 - \left[\left(\frac{bJ(J+1)}{2}\right)^4 + \left(\frac{bJ(J+1}{3}\right)^3\right]^{\frac{1}{2}}\right\}^{\frac{1}{3}}\right). \end{aligned} \tag{19}$$

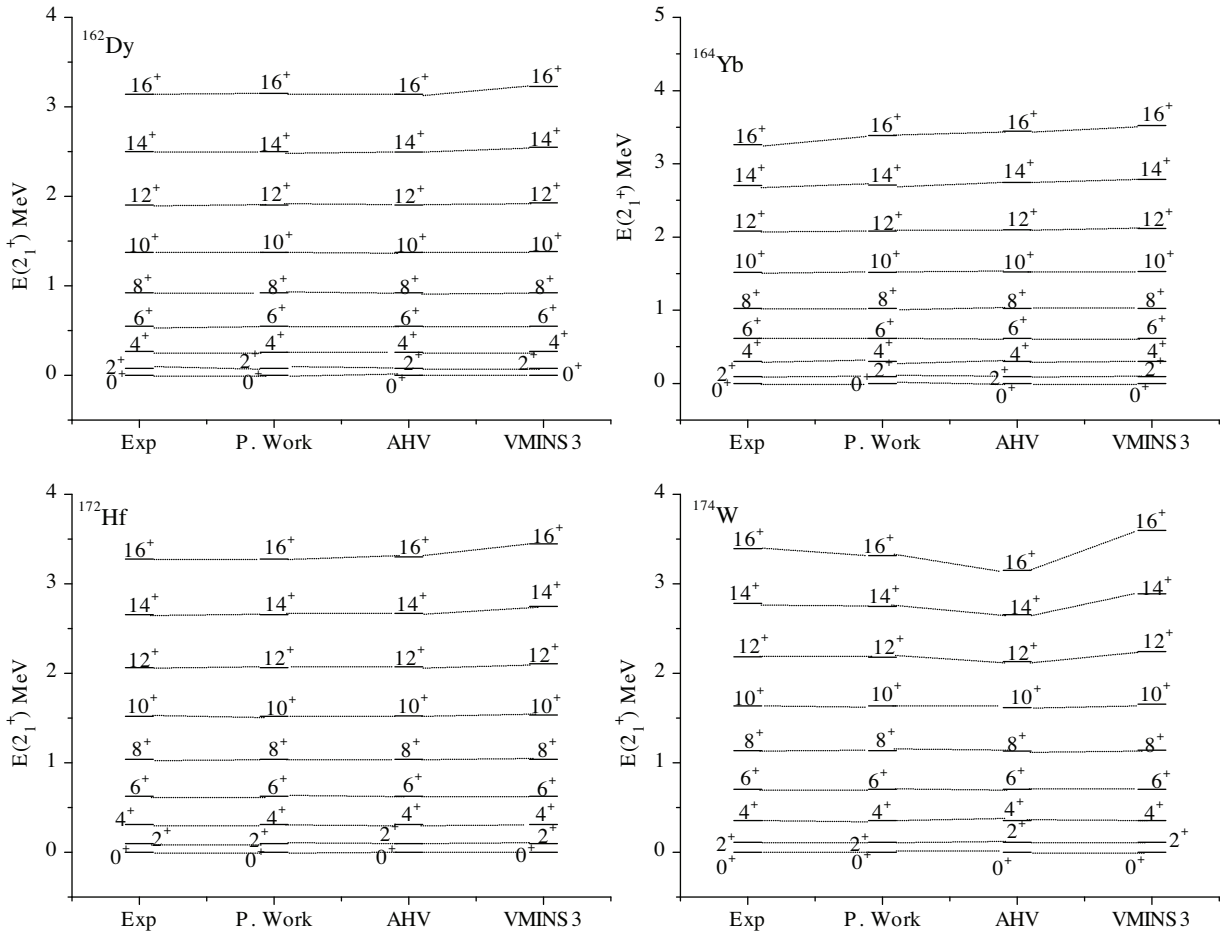

Figure 16. Comparison between experimental energy with anharmonic vibrator expression (AHV), VMINS3 model and p. work.

Zeng et al. [29] gave an alternative derivation of equation (19) from the hydrodynamic model. In this model the energy of a rotating nucleus is given by the relation

$$E(J) = \frac{J(J+1)}{2\beta_J} + \frac{1}{2}C(\beta_J - \beta_0)^2. \tag{20}$$

Batra and Gupta [17] proposed a modified version of equation (20) called the VMINS3 model and derived from the scaling parameter β_J in which the solution of equation (20) is also involved, i.e,

$$\beta_J = \beta_0(1 + \sigma_1 J + \sigma_2 J^2 + \cdots). \tag{21}$$

By limiting to the softness parameter σ_1 in the first approximation, they obtained the expression

$$E(J) = \frac{J(J+1)}{2\beta_0(1+\sigma_1 J)} + P\sigma_1^2 J^2. \tag{22}$$

With $P = \frac{1}{2}C\beta_0^2$ from equation (5),

$$E(J) = (a + cJ)J(J+1) + bJ, \tag{23}$$

the first approximation reduces to

$$E(J) = \frac{aJ(J+1)}{(1+\sigma J)} + bJ, \qquad \text{where} \quad \sigma = -\text{c/a}. \tag{24}$$

The constants a, b and c of both equations are calculated by least squares method. Both equations give better fit with less average deviations. Results obtained from these equations and by fitting the parameters are summarized in Figures 15 and 16. The scaling of J can be obtained in the VMI model through varying β_J. Similar results are obtained for Bohr-Mottelson expression (equation (5)) by varying the contribution of three parameters. Thus, the Bohr-Mottelson expression is more accurate than the VMINS3 equation.

5. Conclusions

Relative ROTE/$E(2_1^+)$ and relative VIBE/$E(2_1^+)$ energies exhibit trends opposite of one another. The axially γ-rigid region lies between the anharmonic vibrator limit U(5) and the axially symmetric rotor limit SU(3) of IBM-1. This is also the region which has been described by the critical point symmetry X(5). The plot of ROTE/$E(2_1^+)$ vs. γ_0 is scattered in the region $N < 82$, but in other three regions there is exponential fall, hence saturations attained with different intercepts and slopes. Therefore, the above mentioned formulae help to explain the structure of nuclei implying that ROTE/$E(2_1^+)$ does not decrease with—but VIBE/$E(2_1^+)$ decreases with deformation.

When we correlate β and γ_0 to one another, we obtain a one parameter description of nuclear shapes. In a complementary way both show decrease in energy; but in $R_{4/2}$ their relative contribution decreases and increases in complementary way which becomes more informative.

We also find the odd-even staggering (OES) in the γ-bands helps to distinguish between its rigid triaxial rotor and γ-soft. We have used the SRF formula to identify the nature of the nuclei by considering $^{122\text{–}124}$Xe and $^{124\text{–}128}$Ba isotopes. $^{122\text{–}124}$Xe isotopes show the triaxial nature and $^{124\text{–}128}$Ba isotopes show the γ-soft behavior. Thus, the present study taken for $^{122\text{–}124}$Xe and $^{124\text{–}128}$Ba nuclei shows a wide ranging applicability of the above approach.

References

[1] A. Bohr and B. R. Mottelson, *Nuclear Structure W. A. Benjamin, Inc., New York*, **II**, (1975), 145.

[2] T. K. Das, R. M. Dreizler and A. Klein, *Phys. Rev.*, **2**, (1970), 632.

[3] T. K. Das, *Phys. Lett.*, **34B**, (1971), 299.

[4] E. Ejiri, M. Ishihara, M. Sakai, K. Katori and J. Inamura, *J. Phys. Soc. (Japan)*, **24**, (1968), 1189.

[5] J. B. Gupta, H. M. Mittal and S. Sharma, *Physica Scripta*, **41**, (1990), 660.

[6] C. A. Mallmann, *Phys. Rev. Lett.*, **2**, (1959), 507.

[7] J. B. Gupta and A. K. Kavathekar, *Physica Scripta*, **56**, (1997), 574.

[8] A. S. Davydov and G. F. Filippov, *Nucl. Phys.*, **8**, (1958), 237.

[9] A. S. Davydov and V. S. Rostovsky, *Nucl. Phys.*, **12**, (1959), 58.

[10] M. Singh et al., *Can. J. Phys.*, **85**, (2007), 889.

[11] M. Singh et al., *Adv. Studies Theor. Phys.*, **3**, (2009), 251.

[12] E. A. McCutchan et al., *Phys. Rev. C*, **76**, (2007), 024306.

[13] N. V. Zamfir and R. F. Casten, *Phys. Lett. B*, **260**, (1991), 265.

[14] Z. J. Liao, *Phys. Rev. C*, **51**, (1995), 141.

[15] P von. Brentano et al., *Phys. Rev. C*, **69**, (2004), 044314.

[16] http: // www.nndc.bnl.gov/

[17] J. S. Batra and Raj K. Gupta, *Phys. Rev. C*, **43**, (1991), 1725.

[18] M. A. J. Mariscotti, G. Scharff-Goldhaber and B. Buck, *Phys. Rev.*, **178**, (1969), 1864.

[19] Y. P. Varshni and S. Bose, *Nucl. Phys. A*, **144**, (1970), 645.

[20] J. Meyer-Ter Vehn, *Nucl. Phys. A*, **249**, (1975), 111.

[21] K. K. Gupta, V. P. Varshney and D. K. Gupta, *Phys. Rev. C*, **26**, (1982), 685.

[22] D. M. Van Patter, *Nucl. Phys.*, **14**, (1959), 42.

[23] L. Grodzins, *Phys. Lett.*, **2**, (1962), 88.

[24] F. Iachello and A. Arima, *The Interacting Boson model*, (Cambridge University Press, Cambridge. 1987).

[25] L. Esser, U. Neuneyer, R. F. Casten and P von. Brentano, *Phys. Rev. C*, **55**, (1997), 206.

[26] G. Thiamova, *The European Physical Journal A*, **45**, (2010), 81.

[27] L. Wilets and M. Jean, *Phys. Rev.*, **102**, (1956), 788.

[28] P. Holmberg and P. O. Lipas, *Nucl. Phys. A*, **117**, (1968), 552.

[29] Guo-Mo-Zeng, Wei Liu and En-Guang Zhao, *Phys. Rev. C*, **52**, (1995), 1864.